THE EFFECTS OF BED SLOPE AND WAVE SKEWNESS ON SEDIMENT TRANSPORT AND MORPHOLOGY

D.J.R. Walstra[1,2], L.C. van Rijn[1,3], M. van Ormondt[1], C. Brière[1], A.M. Talmon[1,4]

1. WL | Delft Hydraulics, P.O. Box 177, 2600 MH Delft, The Netherlands, Dirkjan.Walstra@wldelft.nl, Leo.vanRijn@wldelft.nl, Maarten.vanOrmondt@wldelft.nl, Christophe.Briere@wldelft.nl, Arno.Talmon@wldelft.nl
2. Delft University of Technology, Faculty of Civil Engineering and Geosciences, P.O. Box 5048, 2600 GA Delft, The Netherlands.
3. Utrecht University Department of Physical Geography, Faculty of Geosciences, P.O. Box 80.115, 3508 TC Utrecht, Netherlands.
4. Delft University of Technology, Faculty of Mechanical, Maritime and Materials Engineering, Mekelweg 2, 2628 CD Delft, The Netherlands.

Abstract: The potential relevance of wave skewness and sloping beds on morphodynamic predictions is investigated. Based on a comparison with measurements it was shown that the phase lag is potentially important for modeling nearshore bar dynamics as it influences the suspended wave related transports (magnitude and direction). Velocity skewness results in a phase shift between the orbital motion and the instantaneous bed shear stress increasing onshore bed load transport. It was seen that its influence is relatively small but does affect bar migration and helps to predict the observed asymmetric bar shape. The bed slope affecting the initiation of motion and sediment bed-load transport magnitude and direction are investigated by comparing scour hole predictions. The initiation of motion, which is also included on the suspended transports, only has an effect for somewhat steeper slopes. The modifications of bed-load direction and magnitude significantly affect the horizontal and vertical scour hole equilibrium dimensions.

INTRODUCTION

As part of the implementation of the TR2004 transport formulations (Van Rijn, 2006a,b)

in the Delft3D-Online model (Lesser et al., 2004) a number of additional processes were included or updated. Here we are focusing on processes of which the relative importance in morphodynamic simulations is not well known. The investigated processes are the phase lag effects on the wave related suspended transport, the role of orbital velocity skewness on the bed shear stress and the effect of sloping beds on bed-load and suspended sediment transport. First, a brief description of the considered processes is given, followed by a limited number of morphodyamic simulations to illustrate their potential relevance. Finally, some concluding remarks and recommendations for further research are given.

PHASE LAG EFFECTS

The wave-induced suspended transports are based on an intra-wave approach, which consists of a parameterized description of the instantaneous response of the suspended sand concentration to the near-bed orbital wave motion (Houwman and Ruessink, 1996):

$$q_{s,w} = \lambda f_p \left(\frac{U_{on}^4 - U_{off}^4}{U_{on}^3 + U_{off}^3} \right) \int_a^{3\delta_s} c\,dz \qquad (1$$

in which U_{on} is the near-bed peak orbital velocity in onshore direction (in wave direction), U_{off} is the near-bed peak orbital velocity in offshore direction, c the vertical distribution of the time-averaged sediment concentration, λ is a coefficient (0.1), d_s is the thickness of the wave boundary layer, an extension of the original formulation is the function (f_p) which represents the phase-lag effects.

Phase lag effects may occur when sediment is stirred up and does not respond directly to the orbital wave motion as it takes time to fall back to the bed (Dohmen-Janssen, 1999). The phase lag can result in a decreased transport of sediment in the wave direction or can, in cases of fine sediment and relative short wave periods, result in sediment being transported against the wave propagation direction. Van Rijn (2006b) accounted for this phase-lag effect by including a f_p-phase function ($-1 < f_p < 1$) which depends on the bed characteristics (form roughness, grain size) and the strength of the asymmetric wave motion:

$$f_p = -\tanh\left[100\left(P - P_{cr}\right)\right]$$

with $P = \dfrac{k_s}{w_s T_p}$, in which k_s is the wave-related bed roughness height, w_s is the settling velocity, T_p is the peak wave period, and P_{cr} is the critical phase lag number which is set to 0.1.

WAVE SKEWNESS

Nielsen (1992, 2002, 2006) and Nielsen and Callaghan (2003) have shown that fluid accelerations in strongly asymmetric wave motion lead to an increase and phase lead of the bed-shear stresses. This is partly due to the presence of boundary layer streaming and partly to the saw-tooth asymmetry, i.e. the front of the waves being steeper than the back. Moreover, Watanabe and Sato (2004) have shown that the fluid acceleration effects on the bed shear stresses leads to a small net transport in the case of forward

leaning waves, even if the peak onshore and offshore orbital velocities are equal, because of the more abrupt acceleration under the steep front. More abrupt accelerations are associated with thinner boundary layers and greater pressure gradients for a given velocity magnitude.

Nielsen and Callaghan (2003) proposed a simple method to deal with these processes, by expressing the transport rate in terms of an instantaneous Shields parameter rather than in terms of a free stream velocity, and accounting for both streaming and accelerations in the Shields parameter calculations. The instantaneous bed-shear stress under asymmetric wave motion including enhanced acceleration effects in saw-tooth waves reads as:

$$\tau'_{b,t} = 0.5\rho_w f'_w \left| u_{w,t}\cos\xi_\tau + \frac{1}{\omega}\frac{du_{w,t}}{dt}\sin\xi_\tau \right| \left(u_{w,t}\cos\xi_\tau + \frac{1}{\omega}\frac{du_{w,t}}{dt}\sin\xi_\tau \right) \quad (3)$$

in which ρ_w is the fluid density, f'_w is the grain-related wave friction factor, $u_{w,t}$ the instantaneous orbital velocity at the edge of the wave boundary layer, ω is the angular wave frequency and ξ_t is the phase lead.

Consequently the instantaneous bed shear stress values shifts forward and the peak bed-shear stress increases with the phase lead-value, leading to an increase of the onshore net transport. Based on comparison with the Watanabe and Sato (2004) experiments, Nielsen (2006) recommends using a phase lead-value of 51°. However, the range of the optimal values is relatively large for considered experiments (average values for ξ_t in the range of 40° to 62°). Here we are driving the Nielsen and Callaghan (2003) model with a velocity signal derived from a non-linear wave model based on Isobe and Horikawa (1982) which only describes velocity skewness. Acceleration skewness which is associated with saw-tooth waves (or pitched-forward waves) is not accounted for.

BED SLOPE EFFECTS

Most transport formulas are only valid for (nearly) horizontal beds (bed slope=tan $\beta \leq 10^{-3}$ (positive values of β refer to down sloping beds). Based on the results of experimental work, it appears that the bed slope may affect the transport rate in three ways:

1. the bed slope will influence the local near-bed flow velocity (hydrodynamic effect not considered here);
2. the bed slope will change the threshold conditions for initiation of motion;
3. the bed slope may change the transport rate and/or direction, once the sediment is in motion.

Here we will discuss expressions dealing with the initiation of motion and the change of transport rate and/or direction and how they are implemented in Delft3D.

Threshold conditions

Dey (2001, 2003) studied the critical bed-shear stress on both longitudinal and transverse (lateral) bed slopes. Experiments were conducted in two different, transparent (perspex) semi-circular ducts for three sizes (600, 940 and 1350 μm with angles of

repose of 32°, 34° and 35°) of uniform sediments. Based on these experiments Dey (2003) derived a rather complicated expression to describe the critical bed-shear stress along combined longitudinal and transverse bed slopes, which reads as:

$$\frac{\tau_{b,cr}}{\tau_{b,cr,o}} = a\left(-b + \left(b^2 + c\right)^{0.5}\right)$$

with $a = \left(\left(1 - \eta \tan\phi\right)\tan\phi\right)^{-1}$, $b = \sin\beta + \eta\left(\tan\phi\right)^2\left(\left(\cos\phi\right)^2 - \left(\sin\phi\right)^2\right)^{0.5}$, $c = \left(1 - \left(\eta\tan\phi\right)^2\right)\left(\left(\cos\phi\tan\phi\right)^2 - \left(\sin\phi\tan\phi\right)^2 - \left(\sin\beta\right)^2 - \left(\sin\gamma\right)^2\right)$, η is the ratio of lift and drag forces on a particle, $\tau_{b,cr}$ is the critical bed-shear stress, $\tau_{b,cr,o}$ is the critical bed-shear stress along the horizontal bed, β is the longitudinal slope angle (positive values refer to down sloping beds), γ is the lateral (transverse) slope angle and ϕ is the angle of repose.

Assuming a horizontal bed in normal to the flow direction ($\gamma = \eta = 0$), Eq. (4) reduces to the Schoklitsch equation. When assuming a horizontal bed in longitudinal direction ($\beta = \eta = 0$) Eq. (4) reduces to the Leitner equation (see e.g. Van Rijn, 1993). Dey showed that Eq. (4) is in reasonable agreement with his experimental values. However, it significantly over-predicts the critical bed shear stress for relatively large longitudinal adverse slopes. Here we are using an empirical expression proposed by Dey (2001) which was modified slightly to improve the agreement with measured data (see Fig. 1):

$$\frac{\tau_{b,cr}}{\tau_{b,cr,o}} = \left(1 - \frac{\tan\beta}{\tan\phi}\right)^{0.75}\left(1 - \frac{\tan\gamma}{\tan\phi}\right)^{0.37} \tag{5}$$

The instantaneous bed load transport due to the combined action of waves and currents is based on Van Rijn (2006a) and reads in simplified form:

$$S_{b,t} = A\left(\frac{\tau_{b,cw,t}}{\rho_w}\right)^{0.5}\left(\frac{\tau_{b,cw,t} - \tau_{b,cr}}{\tau_{b,cr}}\right) \tag{6}$$

in which A is a factor (see Van Rijn; 2006a), $\tau_{b,cw,t}$ is the instantaneous grain-related bed-shear stress due to both currents and waves.

From Eq. (6) it becomes clear that the threshold condition, Eq. (5), will result in a linear scaling of the bed load transports.

The modification of the critical bed shear is also applied on the reference concentration, c_a, (Van Rijn, 2006b):

$$c_a = B\left(\frac{\overline{\tau}_{b,cw} - \tau_{b,cr}}{\tau_{b,cr}}\right)^{1..5}$$

in which B is a factor (see Van Rijn, 2006b), $\overline{\tau}_{b,cw}$ is the time-averaged effective bed-shear stress and $\tau_{b,cr}$ is the critical bed-shear stress according to Shields including the modification of the threshold condition according to Eq. (5).

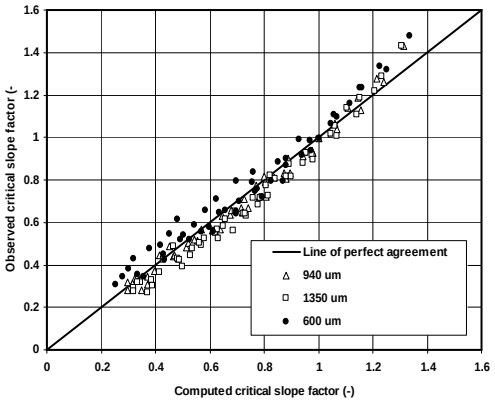

Fig. 1 Observed and computed critical slope factor for combined longitudinal and transverse bed slopes based on Eq. (5) modified expression of Dey (2001).

Bed load transport on sloping beds

Two methods are considered which describe the transverse transports on a sloping bed. The first method, originating from Van Bendegom (1947), determines the angle of the transverse transports based on the forces acting on a particle along a sloping bottom. The second method (Ikeda, 1988) is based on the equation of motion and results in a correction of the transport magnitude. Both transverse correction methods are combined with longitudinal corrections which are mentioned for completeness sake, but are not the focus of this paper.

Direction based transverse transport correction

Van Bendegom (1947) gives the following expression for the direction of sediment moving on a sloping bed:

$$\tan\alpha = \frac{S_{b,n}}{S_{b,s}} = \frac{\sin\delta - \frac{1}{f(\theta)}\tan\gamma}{\cos\delta - \frac{1}{f(\theta)}\tan\beta} \tag{8}$$

in which $S_{b,n}$ and $S_{b,s}$ are the bed load transports in transverse and longitudinal direction respectively, $f(\theta)$ is a transverse bed-slope coefficient, being a function of the shields number, θ; z_b is the bed elevation, x and y are the horizontal coordinates, d is the angle of the flow near the bed.

Ignoring the longitudinal bed slope effects ($\delta = 0$ and $\tan\beta = 0$) reduces Eq. (8) to:

$$\tan\alpha = -\frac{1}{f(\theta)}\tan\gamma$$

Talmon (1992) and Talmon et al. (1995) studied the direction of sediment transport (bed load and suspended load) on transverse alluvial bed-slopes based on Eq. (9). Laboratory experiments with transverse bed slopes in a straight flume were performed. Various sand sizes were used (d_{50} of 90, 160 and 790 μm). Suspended load transport was dominant in the tests with the finer sediments (90 and 160 μm). The initial bed was placed under a

transverse slope in the (straight) flume. The bed level difference between the left and right sides of the bed in the flume was observed to be smoothed out (leveled) by the flow as a function of time by transverse sediment transport processes. The observed bed development in the experiments with coarse sand (790 μm) can be represented quite well by a relatively simple mathematical model for the transverse sediment transport processes, in which the *f(θ)*-coefficient is represented as (Koch and Flokstra, 1981):

$$f(\theta) = 1.7\theta^{0.5}$$

In the modeling of the bed slope effects in the presence of suspended load transport, it was assumed that only the bed-load transport part of the sediment transport is affected by the transverse sloping bed. In the experiments with fine sediment (90 and 160 μm) the *f(θ)*-values derived from the experimental results are significantly lower (a factor 1.4 for 90 μm sand to 3.5 for 160 μm sand) than the values predicted by Eq. (10). Considering measured data and numerical simulation results of both natural rivers and laboratory flumes, Talmon et al. (1995) have found a distinct influence of the bed forms which differ in both situations (scale effects, particle size and flow depth). This effect can be expressed through the relative particle size (d_{50}/h) as:

$$f\left(\theta, \frac{d_{50}}{h}\right) = 9\left(\frac{d_{50}}{h}\right)^{0.3}\theta^{0.5} \qquad (1$$

This expression suggests that, at the same θ, the transverse slope effect (i.e. *1/f(θ)*) on the bed load transport particles is stronger (smaller *f(θ)*) in situations with finer sediment (dominant suspended load transport) than with dominant bed-load transport, as found in the laboratory experiments with 790 μm. However, the transverse slope effect may also be acting on the suspended particles (at least those close to the bed). This latter approach yields a larger effect in the case of dominant suspended load transport. Talmon (1992) has also studied the morphological behavior of river bends in the case of dominant suspended load transport (>50%). His mathematical model was formulated in terms of the depth-averaged equations using an asymptotic approximation to represent the horizontal and vertical adjustment of the depth-averaged sediment concentration to changing flow conditions (Galappatti-method). Experiments in a curved laboratory flume have been conducted to provide verification data for the mathematical model. The effect of transverse bed slopes is assumed to act on the bed load transport fraction only. Using this approach, the transverse bed slopes are under-predicted by the model. This suggests that either the *f(θ)*-value acting on the bed load transport fraction is too small or it should also be applied to the suspended load particles.

The approaches described by Eqs. (10) and (11) are combined with a longitudinal slope effect based on Koch and Flokstra (1981) which reads:

$$\alpha_s = 1 + \varepsilon_s \tan\beta$$

in which e_s is a user-specified tuning parameter (default value: 0.05)

Talmon (1992) used this parameter in various comparisons with experiments and used values for e_s in the range of 0.15 to 0.3.

Magnitude based transverse transport correction

An alternative approach is based on the equation of motion of a particle moving over a sloping bed, suggested by Ikeda (1988) for transverse sloping beds:

$$\alpha_n = \varepsilon_n \left(\frac{\tau_{b.cr}}{\tau_b} \right)^{0.5} \tan\gamma$$

in which ε_n is a user-specified tuning parameter (default value: 1.5, range between 1.5 and 3).

Lesser et al. (2004) used Ikeda (1988) to model the morphological development (dominant bed load transport; sediment of 450 μm; mean velocity of 0.4 m/s) of a river bend in a laboratory flume. Good results were obtained by using ε=2.

The Ikeda (1988) method is combined with the Bagnold (1956) approach for longitudinal sloping beds:

$$\alpha_s = 1 + \varepsilon_s \left(\frac{\tan\phi}{\cos\left(\tan^{-1}\beta\right)\left(\tan\phi - \tan\beta\right)} - 1 \right) \tag{14}$$

in which e_s is a user-specified tuning parameters (default value: 1).

Implementation in Delft3D

Both methods to account for sloping beds (van Bendegom and Ikeda) in the bed load transport are included in Delft3D. In both methods first the *magnitude* of the transport is determined or modified by applying the longitudinal bed slope correction factor, next the *direction* of the transport is modified by applying the transverse bed slope correction factor. However, due to the way how the bed slope adjustment factors have been derived, the implementations in Delft3D differ slightly for both methods. The description given here is based on a vectoral description of transports in the horizontal plane.

For the Ikeda/Bagnold method the implementation is based on:

$$\begin{aligned} S'_{b,x} &= \alpha_s S_{b,s} \cos\alpha - S_{b,n} \sin\alpha \\ S'_{b,y} &= \alpha_s S_{b,s} \sin\alpha + S_{b,n} \cos\alpha \end{aligned} \tag{15}$$

in which $S'_{b,x}$ and $S'_{b,y}$ are the adjusted bed-load transport components based on the unadjusted transports $S_{b,s\ or\ n}$ and α_s is determined according to Eq. (14).

By using $S_{b,n} = \alpha_n |S_b|$, $\sin\alpha = \frac{S_{b,y}}{|S_b|}$ and $\cos\alpha = \frac{S_{b,x}}{|S_b|}$, Eq. (15) can be written as:

$$\begin{aligned} S'_{b,x} &= \alpha_s S_{b,x} - \alpha_n \alpha_s S_{b,y} \\ S'_{b,y} &= \alpha_s S_{b,y} + \alpha_n \alpha_s S_{b,x} \end{aligned}$$

For the van Bendegom based methods the bed slope factors are taken into account by first adjusting the magnitude of the bed load transport:

$$S_b^{'} = \alpha_s S_b$$

with α_s according to Eq.(12).

The adjusted transport is subsequently decomposed by using:

$$S_{b,x}^{'} = S_b^{'}\left(\frac{\alpha_{n,x}}{\left(\left(\alpha_{n,x}\right)^2+\left(\alpha_{n,y}\right)^2\right)^{0.5}}\right) \text{ and } S_{b,y}^{'} = S_b^{'}\left(\frac{\alpha_{n,y}}{\left(\left(\alpha_{n,x}\right)^2+\left(\alpha_{n,y}\right)^2\right)^{0.5}}\right) \quad (18)$$

where $a_{n,x}$ and $a_{n,y}$ are the decomposed transverse bed slope factors:

$$\alpha_{n,x} = f(\theta)\frac{S_{b,x}}{S_b}+\frac{dz_b}{dx} \text{ and } \alpha_{n,y} = f(\theta)\frac{S_{b,y}}{S_b}+\frac{dz_b}{dy} \quad (19)$$

with $f(\theta)$ being determined according to Eqs. (10) or (11), note that in the above equation the unadjusted transports are used.

MORPHODYNAMIC APPLICATIONS

The aim of this section is to illustrate the relevance of the discussed modifications rather than claiming to provide a comprehensive overview. The selected test cases have the characteristics for which the discussed extensions are potentially important. The phase lag and wave skewness are investigated for the LIP11D experiments carried out in WL | Delft Hydraulics' Delta flume (Arcilla et al., 1994). Using a water depth of 4.1 m, the length of the constructed bottom profile was approximately 180 m. Here both the erosive (Test 1B: H_{m0} = 1.4 m, T_p = 5 s) and accretive (Test 1C: H_{m0} = 0.6 m, T_p = 8 s) test are considered. The predicted and measured profile development are compared after 18 (Test 1B) and 13 hours (Test 1C), with a focus on the bar at x=138 m.

Phase lag effects

Three runs were carried out: f_p was determined using Eq. (2) and setting it to -1 and +1, representing its maximum offshore and onshore limits. The profile developments are compared in Fig. 2 for both tests. It is clear that the wave suspended transport is able to change the direction of the bar migration. The value for f_p according to Eq. (2) is close to +1 which correctly predicts the shoreward or seaward bar migration. However, for Test 1B the λ was set to 0.03 (compared to 0.1 for Test 1C) in Eq. (1).

Wave skewness

A sensitivity analysis was performed by varying the phase lead, ξ_t, in the range of [0°, 10°, 25°, 40°, 51°]. The results are shown in Fig. 3, from which is becomes apparent that ξ_t only results in a visible influence when it is 25° or larger. The higher ξ_t-values enhance the bed-shear stress, increasing of the onshore net transport. The best agreement is obtained for the ξ_t ranging from 25° to 40°. The observed onshore bar migration which is accompanied with enhanced asymmetry bar shape is qualitatively reproduced by the model using the higher ξ_t-values for Test 1C. Furthermore, ξ_t mainly affects the bar regions. The inner bars that are predicted in both tests are not realistic and are mainly due to the applied relatively simple orbital motion model which does not account

for the fact that waves evolve from peaked waves (shoaling) to asymmetric pitched-forward shapes with steep front faces after breaking (Hoefel and Elgar, 2003). This essentially results in a transition from velocity skewness to acceleration skewness being dominant. This is also relevant for the phase lag results discussed in the previous section.

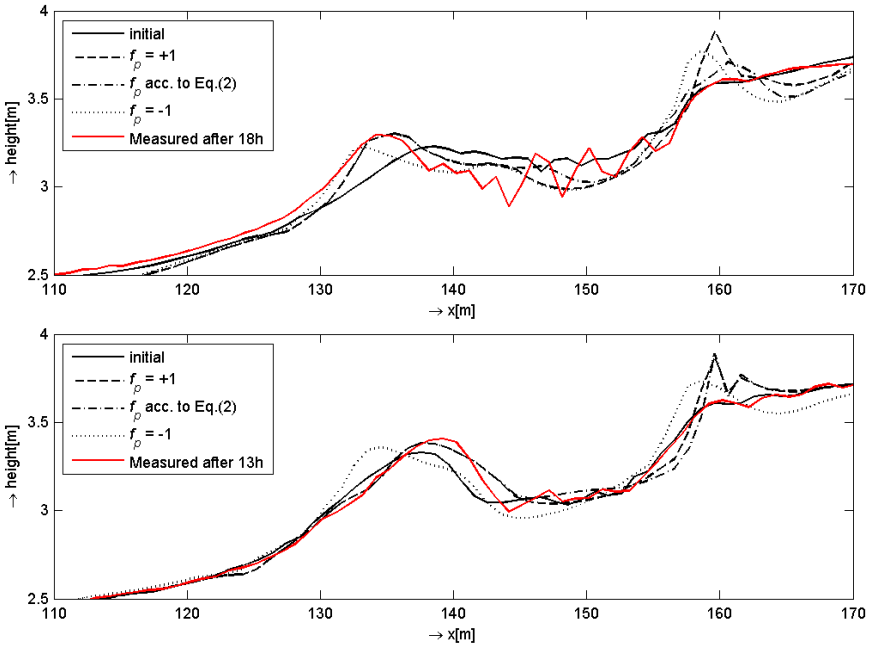

Fig. 2 Profile development induced by various settings of the f_p phase-factor for LIP11D Test 1B (top) and Test 1C (bottom).

Bed slope effects

To illustrate the influence of the discussed slope corrections, transverse and longitudinal transports are compared as a function of the shields parameter for a horizontal bed and two transverse bed slopes ($\tan\gamma = 0.05$ and $\tan\gamma = 0.2$) at 5 m water depth and d_{50} is 0.2 mm. Only transverse bed slopes are considered (i.e. horizontal longitudinal bed). Furthermore, their influence is investigated by comparing the morphodynamic predictions for a schematic case in which, due to current contraction, a scour hole develops.

First the modification of the initiation of motion (Dey, 2001) is investigated by comparing the resulting transports including and excluding Dey (2001) in combination with Ikeda (1988). The transverse bed-load transports are shown in Fig. 4, from which it can be seen that Dey (2001) results in an overall transport increase for the large slope case (compare the blue and the dashed-black lines). For the mild slope Dey (2001) has no visible influence (compare red and solid-black lines). Similar trends are visible for the longitudinal transports shown in Fig. 5.

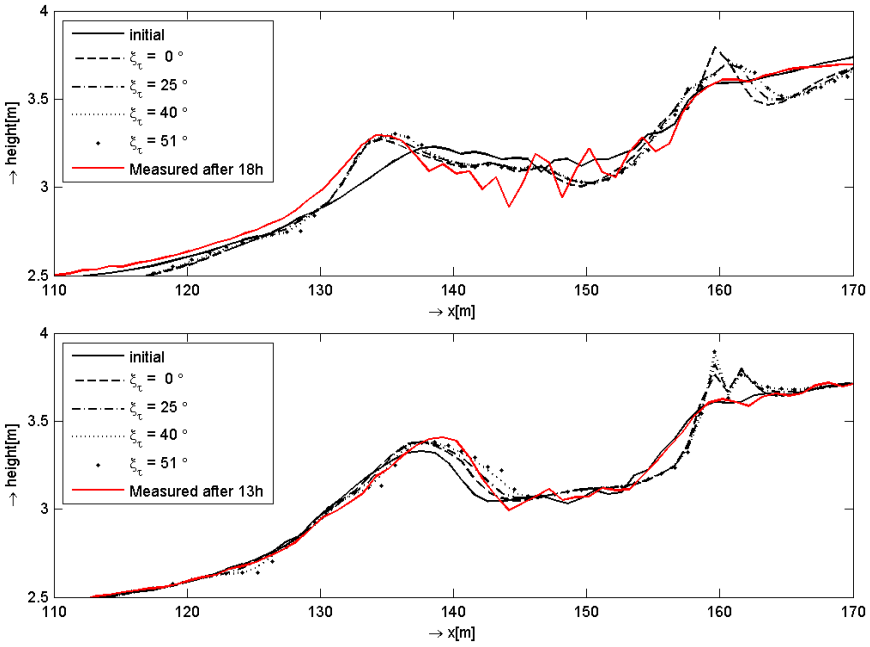

Fig. 3 Profile development induced by various settings of the phase lead for LIP11D Test 1B (top) and Test 1C (bottom).

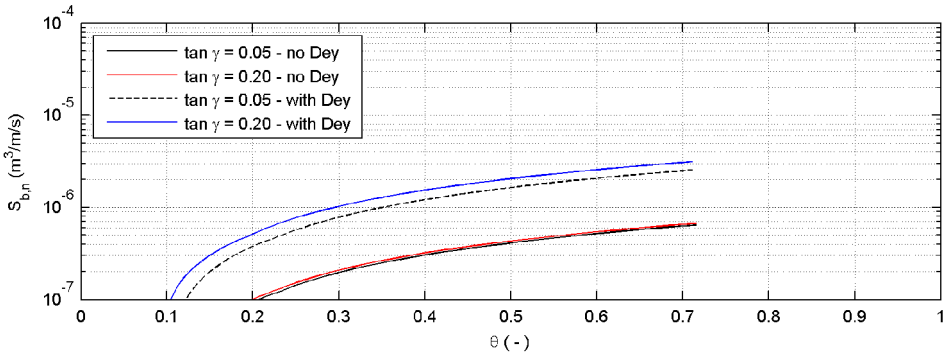

Fig. 4 Transverse bed-load transport as a function of the shields parameter for various transverse sloping beds.

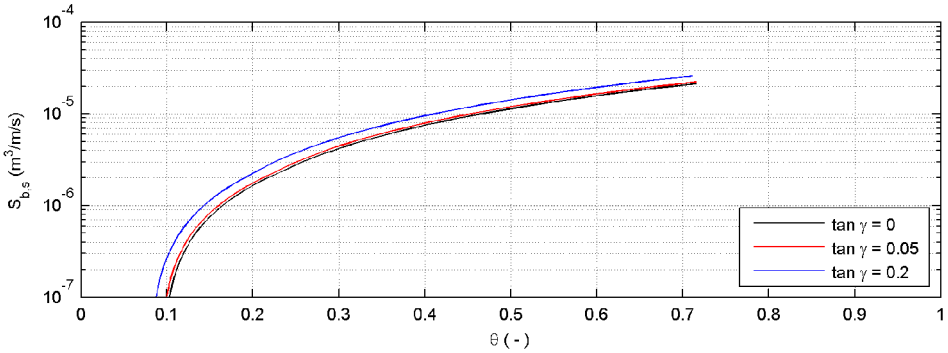

Fig. 5 Longitudinal bed-load transport as a function of the shields parameter for various transverse sloping beds.

The effects on the longitudinal suspended transport are shown in Fig. 6. As could be expected the same trend is found again. However, these results also indicate the potential relevance for including slope effects in the suspended transports. This could especially be the case for areas where suspended sediment is dominant (e.g. ebb tidal deltas and estuaries). Although this approach requires further justification and validation, experimental data (Talmon, 1992) seem to justify this method.

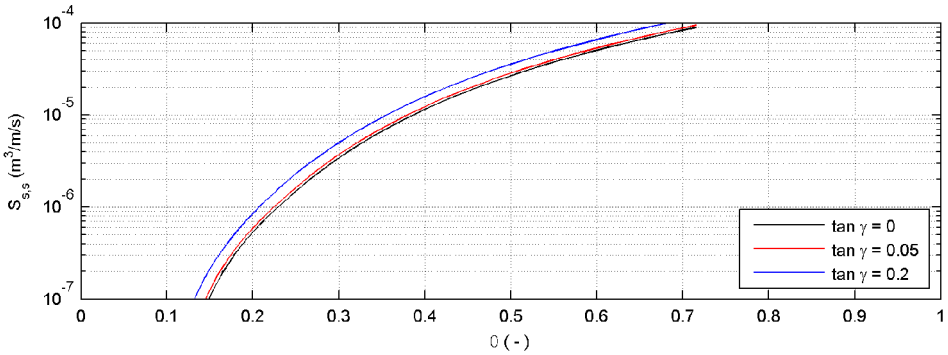

Fig. 6 Longitudinal suspended transport as a function of the shields parameter for various transverse sloping beds.

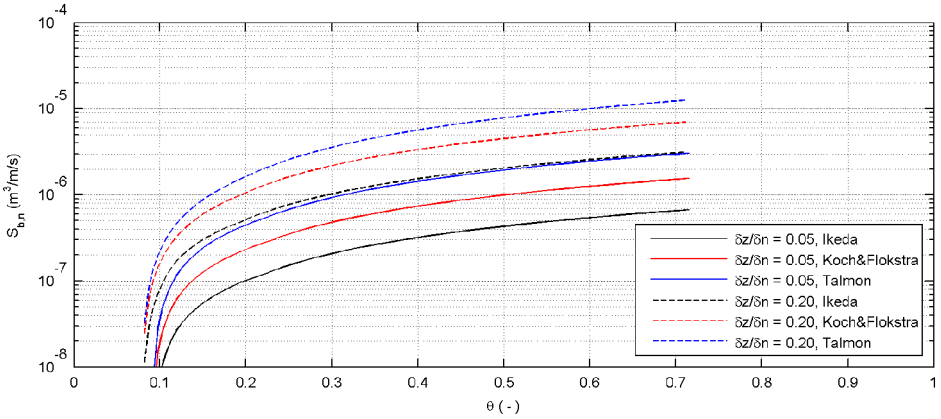

Fig. 7 Transverse bed-load transport as a function of the shields parameter for various transverse sloping bed correction methods.

The transverse bed slope correction methods are compared for the same transverse bed slopes in Fig. 7. The differences between the mild and steep slope transports are of the same order as the differences between the three bed slope correction factors. The behavior of the formulations is very similar, which is somewhat surprising for Ikeda (1988). It was expected for Koch and Flokstra (1981) and Talmon et al. (1995) as they are based on the same approach.

The morphodynamic effects of the different bed slope formulations are investigated by comparing the predictions of a scour hole which is in (near) equilibrium state. The computational grid of the model is 100 m long and 20 m wide with a grid spacing of 1 m in both directions (see Fig. 8) and has an initial uniform water depth of 5 m. Two 4 m long groynes perpendicular to the flow are situated at x = 20 m from the upstream

boundary. A stationary current of 0.5 m/s is imposed at the upstream (left) boundary. Flow contraction results in an initial increase of current velocities up to 0.9 m/s in between the two groynes. The morphodynamic simulations are carried out with the sediment transport relations of Van Rijn (2006a,b) applying a uniform grain size of 0.2 mm. The simulations cover a 100 day period which is sufficiently long to obtain a bathymetry in approximate equilibrium. Three combinations of bed slope formulations are considered, the influence of the initiation of motion (Dey, 2001) is compared in combination with Ikeda (1988) and Talmon et al. (1995) including Dey (2001).

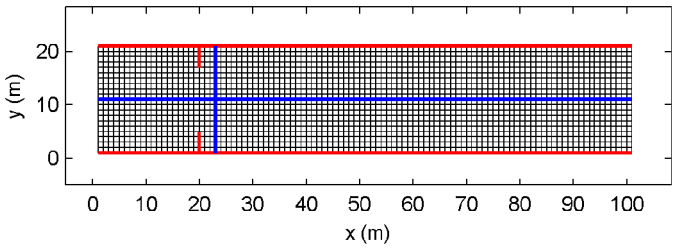

Fig. 8 Grid schematisation including groynes (red) and output transects (blue).

Due to the increased current velocities, a scour hole develops with a depth in the range 6.5 m to 7.2 m depending on the applied bed slope correction formulation as can be seen in Fig. 9. The predicted transverse profiles show a marked difference. Especially the difference between Ikeda (1988) and Talmon et al. (1995) is relatively large.

CONCLUSIONS

The wave-related suspended transport contribution is usually directed in the wave propagation direction, but may, depending on local wave and ripple characteristics, change sign. This transport can be of great importance when modeling morphodynamics in the surf zone, as it can alter the bar migration direction. However, the f_p-phase lag function was not tested extensively and will require further research to assess the robustness of the suggested approach.

Application of the Nielsen and Callaghan (2003) model to account for velocity acceleration in the bed shear stress showed that its effect is relatively small for the considered cases. However, the qualitative trends in bar shape improved with this expression. The best agreement between the model and the observations is obtained for a phase angle, ξ_t, ranging from 25° to 40°. Including acceleration skewness in the orbital velocity signal may improve predictions in the inner (or saturated) surf zone as acceleration skewness tends to be dominant compared to the velocities skewness in this region. This will not only influence the bed-load transports, but may also affect the wave-related suspended transport.

The applied bed slope effects show the expected trends, but the differences between the considered transverse bed slope correction factors is relatively large and results in distinctly different equilibrium bathymetries for the considered case. In combination with recently acquired data on 250 and 960 µm sand, Talmon and Wiesemann (2006) focused on the mechanical balance of moving bed-load particles. In that approach the

shear stress-to-the-grains θ' is the governing variable, instead of θ. Further research will include this new data and the suggested alternative approach. The inclusion of the initiation of motion in both the bed-load and suspended load transport seems conceptually correct, but requires further research. This is emphasized in view of its importance in the predicted equilibrium bathymetries.

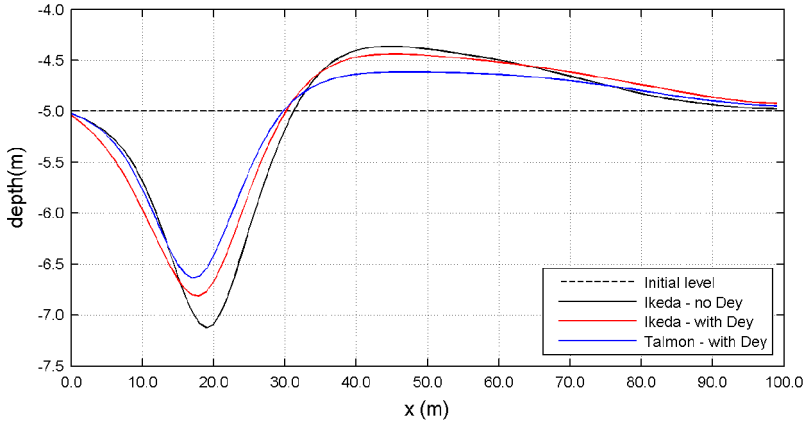

Fig. 9 Resulting longitudinal bottom profiles (y = 10 m) after 100 days.

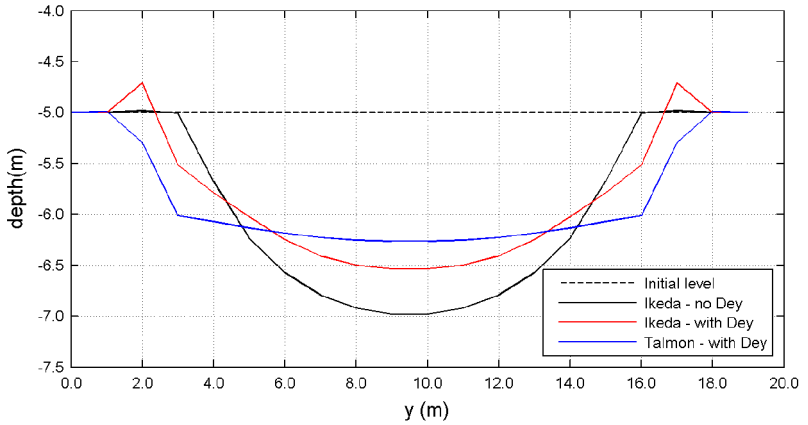

Fig. 10 Resulting transverse bottom profiles (x = 23 m) after 100 days.

REFERENCES

Arcilla, A.S., J.A. Roelvink, B.A. O'Connor and J.A. Jimenez, 1994. The Delta flume '93 experiment, Proc. Int. Coastal Dynamics Conference, Barcelona, pp. 488-502.

Bagnold, R.A., 1956. The Flow of Cohesionless Grains in Fluids. Proc. Royal Soc. Philos. Trans., London, Vol. 249.

Dey, S., 2001. Experimental study on incipient motion of sediment particles on generalized sloping fluvial beds. Int. Journal of Sediment Research, Vol.16, No. 3, p. 391-398

Dey, S., 2003. Threshold of sediment motion on combined transverse and longitudinal sloping beds. Journal of Hydraulic Research, Vol. 41, No. 4, p. 405-415.

Dohmen-Janssen, M., 1999. Grain size influence on sediment transport in oscillatory

sheet flow. Doctoral Thesis. Delft University of Technology, Delft, The Netherlands.
Hoefel, F., and S. Elgar, 2003. Wave-induced sediment transport and sandbar migration, 781 Science, 299, 1885–1887.
Ikeda, S., 1982. Lateral Bed-Load Transport on Side Slopes. Journal Hydraulics Division, ASCE, Vol. 108, No. 11.
Ikeda, S., 1988. Lateral Bed Load Transport on Side Slopes. In: Civil Engineering Practice 2, Technomic Publishing Company, USA.
Isobe, M. and Horikawa, K., 1982. Study on water particle velocities of shoaling and breaking waves. Coastal Eng. in Japan, 25, pp. 109-123.
Koch, F.G. and Flokstra, C., 1981. Bed level computations for curved alluvial channels. 19th IAHR congress, Vol. 2, New Delhi, India.
Lesser, G.R., Roelvink, J.A., Van Kester, J.A.T.M. and Stelling, G.S., 2004. Development and validation of a three-dimensional morphological model. Coastal Engineering, Vol. 51, p. 883-915.
Nielsen, P., 2002. Shear stress and sediment transport calculations for swash zone modeling. Coast Eng. 45, 53-60.
Nielsen, P., 2006. Sheet flow sediment transport under waves with acceleration skewness and boundary layer streaming. Coast. Eng. 53, 749-758.
Nielsen, P. and Callaghan, D.P., 2003. Shear stress and sediment transport calculations for sheet flow under waves. Coast. Eng. 47, 347-354.
Talmon, A.M., 1992. Bed topography of river bends with suspended sediment transport. Doctoral Thesis. Delft University of Technology, Delft, The Netherlands.
Talmon, A.M., Van Mierlo, M.C.L.M. and Struiksma, N., 1995. Laboratory measurements of the direction of sediment transport on transverse alluvial-bed slopes. Journal of Hydraulic Research, Vol. 33, No. 4, p. 495-517.
Talmon, A.M. and J.-U. Wiesemann, 2006, Influence of grain size on the direction of bed-load transport on transverse sloping beds, Int. Conf. on Scour and Erosion ICSE2006, Amsterdam.
Van Bendegom, L., 1947. Enige beschouwingen over riviermorfologie en rivierverbetering. De Ingenieur, Vol. 59, No. 4, p. 1-11.
Van Rijn, L.C., 1993. Principles of sediment transport in rivers, estuaries and coastal seas. Aqua Publications, The Netherlands (www.aquapublications.nl).
Van Rijn, L.C., 2006a. A unified view of sediment transport by currents and waves, part 1: initiation of motion, bed roughness and bed load transport. Accepted for publication in Journal of Hydr. Engineering.
Van Rijn, L.C., 2006b. A unified view of sediment transport by currents and waves, part 2: suspended transport. Accepted for publication in Journal of Hydr. Engineering.
Watanabe, A., Sato, S., 2004. A sheet flow transport rate formula asymmetric forward leaning waves and currents. Proc. 29th ICCE, Lisbon, World Scientific, pp. 1703–1714.